

Minimal surfaces from circle patterns: Geometry from combinatorics

Alexander I. Bobenko* Tim Hoffmann†

Boris A. Springborn‡

February 8, 2020

1 Introduction

The theory of polyhedral surfaces and, more generally, the field of discrete differential geometry are presently emerging on the border of differential and discrete geometry. Whereas classical differential geometry investigates smooth geometric shapes (such as surfaces), and discrete geometry studies geometric shapes with a finite number of elements (polyhedra), the theory of polyhedral surfaces aims at a development of discrete equivalents of the geometric notions and methods of surface theory. The latter appears then as a limit of the refinement of the discretization. Current progress in this field is to a large extent stimulated by its relevance for computer graphics and visualization.

One of the central problems of discrete differential geometry is to find proper discrete analogues of special classes of surfaces, such as minimal, constant mean curvature, isothermic, etc. Usually, one can suggest various discretizations with the same continuous limit which have quite different geometric properties. The goal of discrete differential geometry is to find a discretization which inherits as many essential properties of the smooth geometry as possible.

Our discretizations are based on quadrilateral meshes, i.e. we discretize parametrized surfaces. For the discretization of a special class of surfaces, it is natural to choose an adapted parametrization. In this paper, we investigate conformal discretizations of surfaces, i.e. discretizations in terms of circles and spheres, and introduce a new discrete model for minimal surfaces. See Figs. 1 and 2. In comparison with direct methods (see, in particular, [15]), leading usually to triangle meshes, the less intuitive discretizations of the present paper have essential advantages: they respect conformal properties of surfaces, possess a maximum principle, etc.

We consider minimal surfaces as a subclass of isothermic surfaces. The analogous discrete surfaces, *discrete S-isothermic surfaces* [4] consist of touching spheres, and of circles which intersect the spheres orthogonally in their points

*Partially supported by the SFB 288 “Differential Geometry and Quantum Physics” and the DFG Research Center “Mathematics for Key Technologies” (FZT 86) in Berlin.

†Supported by the SFB 288 “Differential Geometry and Quantum Physics” and the Alexander von Humboldt Foundation.

‡Supported by the SFB 288 “Differential Geometry and Quantum Physics”.

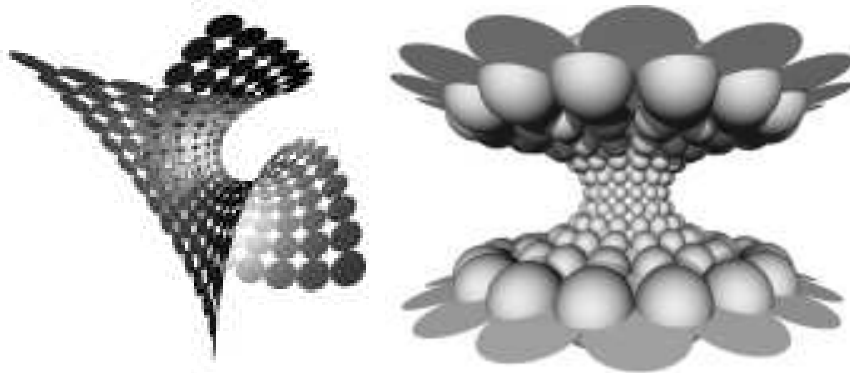
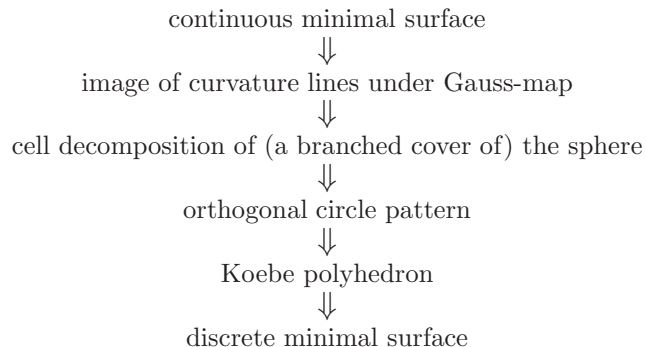


Figure 1: A discrete minimal Enneper surface (*left*) and a discrete minimal catenoid (*right*).

of contact. See Fig. 1 (*right*). Continuous isothermic surfaces allow a duality transformation, the Christoffel transformation. Minimal surfaces are characterized among isothermic surfaces by the property that they are dual to their Gauss map. The duality transformation and the characterization of minimal surfaces carries over to the discrete domain. Thus, one arrives at the notion of *discrete minimal S-isothermic surfaces*, or *discrete minimal surfaces* for short. The role of the Gauss maps is played by discrete S-isothermic surfaces, the spheres of which all intersect one fixed sphere orthogonally. Due to a classical theorem of Koebe (see Section 3) any 3-dimensional combinatorial convex polytope can be (essentially uniquely) realized as such a Gauss map.

This definition of discrete minimal surfaces leads to a construction method for discrete S-isothermic minimal surfaces from discrete holomorphic data, a form of a discrete Weierstrass representation (see Section 8). Moreover, the classical “associated family” of a minimal surface, which is a one-parameter family of isometric deformations preserving the Gauss map, carries over to the discrete setup (see Section 9).

Our general method to construct discrete minimal surfaces is schematically shown in the following diagram. (See also Fig.11.)



As usual in the theory on minimal surfaces [13], one starts constructing such a surface with a rough idea of how it should look. To use our method, one should understand its Gauss map and the *combinatorics* of the curvature line pattern.

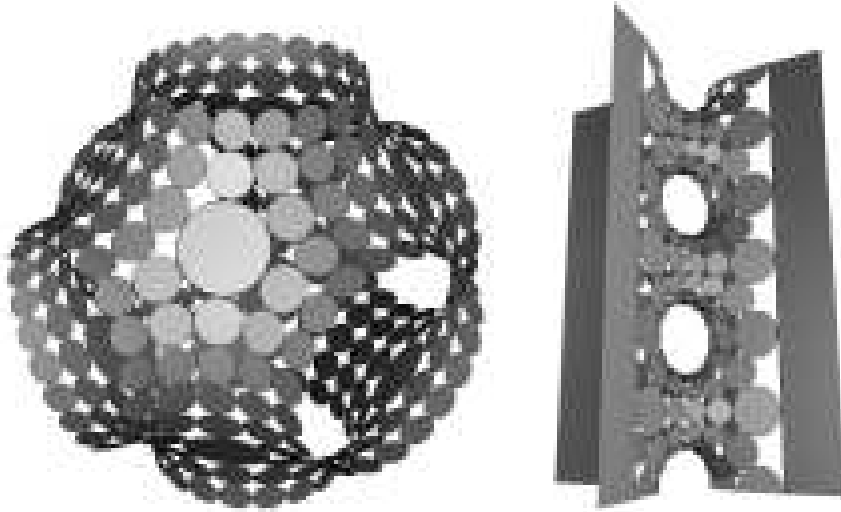


Figure 2: A discrete minimal Schwarz-P surface (*left*) and a discrete minimal Scherk tower (*right*).

The image of the curvature line pattern under the Gauss map provides us with a cell decomposition of (a part of) S^2 or a covering. From these data, applying the Koebe theorem, we obtain a circle packing with the prescribed combinatorics. Finally, a simple dualization step yields the desired discrete minimal surface.

Let us emphasize that our data, besides possibly boundary conditions, are purely combinatorial—the combinatorics of the curvature line pattern. All faces are quadrilaterals and typical vertices have four edges. There may exist distinguished vertices (corresponding to the ends or umbilic points of a minimal surface) with a different number of edges.

The most nontrivial step in the above construction is the third one listed in the diagram. It is based on the Koebe theorem. It implies the existence and uniqueness for the discrete minimal S-isothermic surface under consideration, but not only this. This theorem can be made an effective tool in constructing these surfaces. For that purpose, we use a variational principle from [5] for constructing circle patterns. This principle provides us with a variational description of discrete minimal S-isothermic surfaces and makes possible a solution of some Plateau problems as well.

In the last section of the paper, we prove the convergence of discrete minimal S-isothermic surfaces to smooth minimal surfaces. The proof is based on Schramm’s approximation result for circle patterns with the combinatorics of the square grid [18]. The best known convergence result for circle patterns is C^∞ -convergence of circle packings [12]. It is an interesting question whether the convergence of discrete minimal surfaces is as good.

Apart from discrete minimal surfaces, there are other interesting subclasses of S-isothermic surfaces. In future publications, we plan to treat discrete constant mean curvature surfaces in Euclidean 3-space and Bryant surfaces (these are surfaces with constant mean curvature 1 in hyperbolic 3-space) [7], [10]. More generally, we believe that the classes of discrete surfaces considered in

this paper will be helpful in the development of a theory of discrete conformally parametrized surfaces.

2 Discrete S-isothermic surfaces

We start with the definition and some well known properties of isothermic surfaces.

Definition 1. A surface in 3-space is called *isothermic* if it admits a conformal curvature line parametrization.

Isothermic immersions

$$\begin{aligned} f : \mathbb{R}^2 \supset D &\rightarrow \mathbb{R}^3 \\ (x, y) &\mapsto f(x, y) \end{aligned}$$

are characterized by the properties

$$(1) \quad \|f_x\| = \|f_y\|, \quad f_x \perp f_y, \quad f_{xy} \in \text{span}\{f_x, f_y\}.$$

Geometrically, this definition means that the curvature lines divide the surface into infinitesimal squares. This definition is Möbius invariant, i.e. Möbius transformations of Euclidean 3-space preserve the class of isothermic surfaces. The class of isothermic surfaces includes surfaces of revolution, quadrics, constant mean curvature surfaces, and, in particular, minimal surfaces. We are going to find a proper discrete version of minimal surfaces in this paper characterizing them as a special subclass of isothermic surfaces (see Section 4).

The following definition of discrete isothermic surfaces was already suggested in [3]. It is motivated by the above mentioned geometric interpretation of equations (1). Clearly, the definition is also Möbius invariant.

Definition 2. A polyhedral surface in 3-space is called *discrete isothermic* if all faces are conformal squares.

Conformal squares are circular quadrilaterals with the cross-ratio $= -1$, i.e.

$$\frac{aa'}{bb'} = -1,$$

where a, a', b, b' are the edges of the quadrilateral represented as complex numbers (see Fig. 3). All conformal squares are Möbius equivalent (in particular equivalent to the standard square).

An important fact, which plays a crucial role in our considerations, is the existence of a dual isothermic surface [8].

Proposition 1. Let $f : \mathbb{R}^2 \supset D \rightarrow \mathbb{R}^3$ be an isothermic immersion. Then the formulas

$$f_x^* = \frac{f_x}{\|f_x\|^2}, \quad f_y^* = -\frac{f_y}{\|f_y\|^2}.$$

define an isothermic immersion $f^* : \mathbb{R}^2 \supset D \rightarrow \mathbb{R}^3$ which is called the dual isothermic surface.

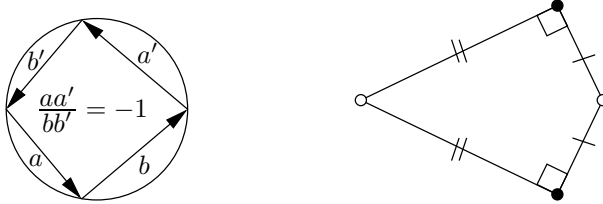


Figure 3: A conformal square (*left*). Right-angled kites are conformal squares (*right*).

Indeed, one can check that the form df^* is closed (and thus defines an immersion) and that f^* satisfies (1). The definition of a discrete dual isothermic surface is based on the same formulas and the proof is elementary.

Lemma 1. *Suppose $a, b, a', b' \in \mathbb{C} \setminus \{0\}$ with*

$$a + b + a' + b' = 0, \quad \frac{aa'}{bb'} = -1$$

and let

$$a^* = \frac{1}{a}, \quad a'^* = \frac{1}{a'}, \quad b^* = -\frac{1}{b}, \quad b'^* = -\frac{1}{b'},$$

where \bar{z} denotes the complex conjugate of z . Then

$$a^* + b^* + a'^* + b'^* = 0, \quad \frac{a^* a'^*}{b^* b'^*} = -1.$$

Proposition 2. *Suppose the edges of a discrete isothermic surface f may consistently be labelled ‘+’ and ‘−’, as in Fig. 4. (For this it is necessary that each vertex has an even number of edges.) Then the dual discrete isothermic surface is defined by the formula*

$$\Delta f^* = \pm \frac{\Delta f}{\|\Delta f\|^2},$$

where Δf denotes the difference of neighboring vertices.

If the edges may not be labelled ‘+’ and ‘−’ consistently, then one can still dualize a suitable covering surfaces which is branched at the vertices of odd degree. This is analogous to the smooth case. Vertices with degree unequal 4 correspond to umbilic points.

The class of discrete isothermic surfaces is too general. Thus, we introduce a more rigid subclass. To motivate its definition, let us look at the problem of discretizing the class of conformal maps

$$f : \mathbb{R}^2 = \mathbb{C} \supset D \rightarrow \mathbb{C}.$$

Conformal maps are characterized by the conditions

$$(2) \quad |f_x| = |f_y|, \quad f_x \perp f_y.$$

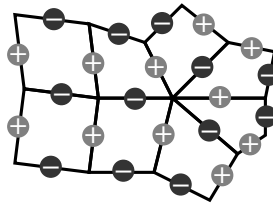


Figure 4: Labelling the edges of a discrete isothermic surface.

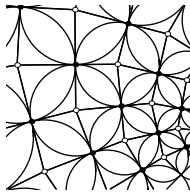


Figure 5: Schramm's circle patterns as discrete conformal maps.

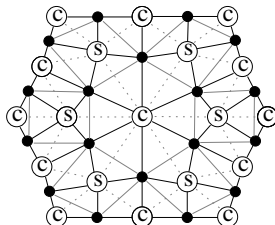


Figure 6: Combinatorics of S-quad-graphs.

To define discrete conformal maps $f : \mathbb{Z}^2 \supset D \rightarrow \mathbb{C}$, it is natural to impose these two conditions on two different sub-lattices (white and black) of \mathbb{Z}^2 , i.e. to require that the edges meeting at a white vertex have equal length and the edges at a black vertex meet orthogonally. This discretization leads to the circle patterns with the combinatorics of the square grid introduced by Schramm [18]. Each circle intersects four neighboring circles orthogonally and the neighboring circles touch cyclically (Fig.5).

A special important subclass of discrete isothermic surfaces called *discrete S-isothermic surfaces* was introduced in [4] as a generalization of Schramm's circle patterns to 3-space. The idea is to replace half of the circles in the above circle pattern by spheres and to generalize the combinatorics.

Before proceeding with the geometric properties, we give a combinatorial description of the discrete surfaces under consideration. A cellular decomposition \mathcal{D} of an oriented two-dimensional manifold (with boundary) is called a *quad-graph*, if all its faces are quadrilaterals. A quad-graph is called *even* if its vertices are colored black or white so that the vertices of each edge have different colors. Such a coloring is always possible for topological discs. Even quad-graphs are in one-to-one correspondence with general cellular decompositions of surfaces. Indeed, let \mathcal{G} be a cellular decomposition of an oriented two-dimensional manifold and \mathcal{G}^* its dual. The faces $F(\mathcal{G})$ of \mathcal{G} are canonically identified with the vertices $V(\mathcal{G}^*)$ of \mathcal{G}^* and vice versa, the edges of \mathcal{G} and \mathcal{G}^* are canonically identified. The union $\mathcal{G} \cup \mathcal{G}^*$ can be also treated as a complex \mathcal{D} called *double*. The set of vertices of the double \mathcal{D} is $V(\mathcal{D}) = V(\mathcal{G}) \cup F(\mathcal{G})$. The edges of \mathcal{D} are defined as connecting the elements of $F(\mathcal{G})$ with their adjacent vertices from $V(\mathcal{G})$. Note that the edges of \mathcal{D} are neither the edges of \mathcal{G} nor of \mathcal{G}^* . The double is an even quad-graph, the vertices $V(\mathcal{G})$ and $V(\mathcal{G}^*) = F(\mathcal{G})$ can be colored black and white respectively.

We impose one further condition of the quad-graphs under consideration. Let us assume that there are also two kinds of white vertices, \textcircled{C} (for circle) and \textcircled{S} (for sphere), such that each quadrilateral of the quad-graph has vertices

of all kinds. See Fig. 6. Such coloring is always possible for topological discs or spheres if each black vertex is of even degree. We call such quad-graphs *S-quad-graphs*.

Definition 3. A *discrete S-isothermic surface* is a mapping

$$f : \mathcal{D} \rightarrow \{\text{curves and spheres with their intersection points in } \mathbb{R}^3\}$$

of an S-quad-graph, such that the images $f(\textcircled{S})$ and $f(\textcircled{C})$ of white vertices are spheres and circles respectively, the images $f(\bullet)$ of black vertices are mapped to their intersection points and the circles and spheres corresponding to the same face of a quad-graph intersect orthogonally.

In some cases the orthogonality condition is automatically satisfied. Consider a sequence of circles C_1, \dots, C_n in 3-space touching cyclically, i.e. the neighboring circles C_i and C_{i+1} as well as C_n and C_1 have common tangents. It is obvious that for $n = 3$ the sphere passing through the touching points of circles crosses them orthogonally. In fact, one can omit the orthogonality condition also in the case $n = 4$ whenever the four circles do not lie on a common sphere.

Lemma 2. (touching coins lemma) *Whenever four circles in 3-space touch cyclically but do not lie on a common sphere, they intersect the sphere which passes through the points of contact orthogonally.*

Given a discrete S-isothermic surface, one can add the centers of the spheres and circles. Consider the following quadrilaterals. The vertices of each are the centers of a sphere and an orthogonal circle together with their points of intersection. These quadrilaterals correspond to the faces of the quad-graph. They are planar and right-angled kites, see Fig. 3 (*right*). Since all such quadrilaterals are conformal squares, we obtain a discrete isothermic surface, which is called the *central extension* of a discrete S-isothermic surface.

The edges of the quad-graph correspond to the edges of the central extension. They are analogous to the curvature lines of a smooth surface. Therefore, typical vertices have four edges. Vertices with a different number of edges model umbilic points. The elements of a discrete S-isothermic surface are shown schematically in Fig. 7.

The following statement, which is also easy to check [4], shows that the duality transformation preserves the class of discrete S-isothermic surfaces.

Proposition 3. *The dual of a central extension of a discrete S-isothermic surface is a central extension of a discrete S-isothermic surface.*

If we disregard the centers, we obtain a definition of a *dual discrete S-isothermic surface*.

The dual discrete S-isothermic surface can be defined without referring to the central extension. Delete the edges of the S-quad-graph incident with the \textcircled{C} vertices to obtain a cellular decomposition \mathcal{G} . Its vertices of it are associated with the spheres and its faces are associated with the original \textcircled{C} vertices, i.e. with the circles of the original discrete S-isothermic surface. The faces are planar, they have inscribed circles and neighboring circles touch. We call this surface *polyhedral discrete S-isothermic surface*. To be able to dualize, the edges

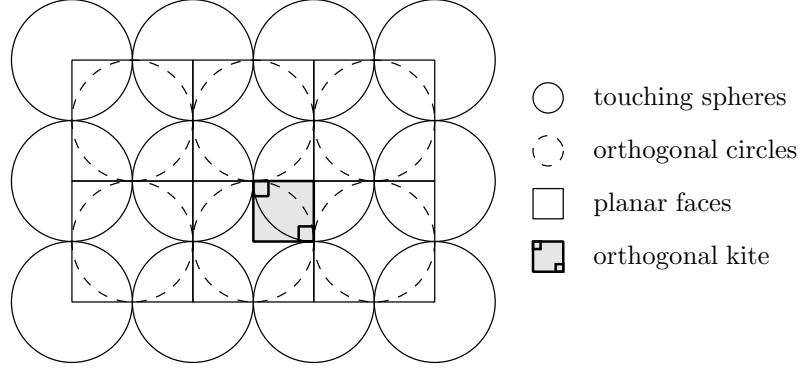


Figure 7: Geometry of a discrete S-isothermic surface without “umbilics”.

of a polyhedral discrete S-isothermic surface have to be labelled ‘+’ or ‘−’ consistently. The following lemma, which follows directly from Lemma 1, describes the dual discrete S-isothermic surface in terms of the corresponding polyhedral discrete S-isothermic surface.

Lemma 3. *Let P be a planar polygon with an even number of cyclically ordered edges given by the vectors $l_1, \dots, l_{2n} \in \mathbb{R}^2$, $l_1 + \dots + l_{2n} = 0$. Suppose the polygon has an inscribed circle with radius R . Let r_j be the distances from the vertices of P to the nearest touching point on the circle: $\|l_j\| = r_j + r_{j+1}$. Then the vectors l_1^*, \dots, l_{2n}^* given by*

$$l_j^* = (-1)^j \frac{1}{r_j r_{j+1}} l_j$$

form a planar polygon with an inscribed circle with radius $1/R$.

Thus the radii of corresponding spheres and circles of a discrete S-isothermic surface and its dual are reciprocal.

3 Koebe polyhedra

In this section we construct special discrete S-isothermic surfaces, which we call the Koebe polyhedra, coming from circle packings (and more general orthogonal circle patterns) in S^2 .

A *circle packing* in S^2 is a configuration of disjoint discs which may touch but not intersect. Associating vertices to the discs and connecting the vertices of touching discs by edges one obtains a combinatorial representation of a circle packing, see Fig. 8 (*left*).

In 1936, Koebe published the following remarkable statement about circle packings in the sphere [14].

Theorem 1. (Koebe) *For every triangulation of the sphere there is a packing of circles in the sphere such that circles correspond to vertices, and two circles touch if and only if the corresponding vertices are adjacent. This circle packing is unique up to Möbius transformations of the sphere.*

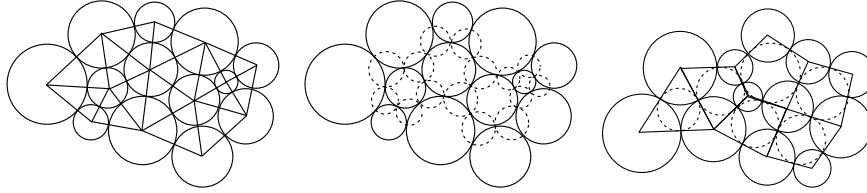


Figure 8: *Left:* A circle packing corresponding to a triangulation. *Middle:* The orthogonal circles. *Right:* A circle packing corresponding to a cellular decomposition with orthogonal circles.

Observe that, for a triangulation, one automatically obtains not one but two orthogonally intersecting circle packings, as shown in Fig. 8 (*middle*). Indeed, the circles passing through the points of contact of three mutually touching circles intersect these orthogonally. This observation leads to the following generalization of Koebe's theorem to cellular decompositions of the sphere with faces which are not necessarily triangular.

Theorem 2. *For every polytopal¹ cellular decomposition of the sphere, there exists a pattern of circles in the sphere with the following properties. There is a circle corresponding to each face and to each vertex. The vertex circles form a packing with two circles touching if and only if the corresponding vertices are adjacent. Likewise, the face circles form a packing with circles touching if and only if the corresponding faces are adjacent. For each edge, there is a pair of touching vertex circles and a pair of touching face circles. These pairs touch in the same point, intersecting each other orthogonally.*

This circle pattern is unique up to Möbius transformations.

The first published statement and proof of this theorem is contained in [6]. For generalizations, see [17], [16], and [5], the latter also for a variational proof (see also Section 6 of this article).

Associating white vertices to circles and black vertices to their intersection points, one obtains a quad-graph. Moreover, exactly four edges meet at each black point. This implies that we have an S-quad-graph, i.e. two kinds of white vertices, \textcircled{S} and \textcircled{C} .

Now let us construct the spheres intersecting S^2 orthogonally along the circles marked by \textcircled{S} . Connecting the centers of touching spheres, one obtains a convex polyhedron, all edges of which are tangent to the sphere S^2 . Moreover, the circles marked with \textcircled{C} are inscribed into the faces of the polyhedron, see Fig. 9. Thus we have a polyhedral discrete S-isothermic surface. The discrete S-isothermic surface is given by the spheres \textcircled{S} and the circles \textcircled{C} .

Thus, Theorem 2 implies the following theorem.

Theorem 3. *Every polytopal cell decomposition of the sphere can be realized by a polyhedron with edges tangent to the sphere. This realization is unique up to projective transformations which fix the sphere.*

There is a simultaneous realization of the dual polyhedron, such that corresponding edges of the dual and the original polyhedron touch the sphere in the

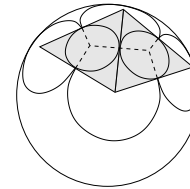


Figure 9: The Koebe polyhedron as a discrete S-isothermic surface.

¹We call a cellular decomposition of a surface *polytopal*, if the closed cells are closed discs, and two closed cells intersect in one closed cell if at all.

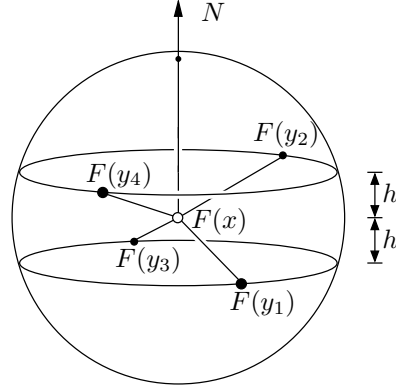


Figure 10: Condition for discrete minimal surfaces.

same points and intersect orthogonally.

The last statement of the theorem follows from the construction if one interchanges \odot and \otimes labels.

4 Discrete minimal surfaces

The following theorem about continuous minimal surfaces, which goes back to Christoffel [8], is the basis for our definition of discrete minimal surfaces.

Theorem 4 (Christoffel). *Minimal surfaces are isothermic. An isothermic immersion is a minimal surface, if and only if the dual immersion is contained in a sphere. In that case the dual immersion is in fact the Gauss map of the minimal surface.*

The idea is to define discrete minimal surfaces as S-isothermic surfaces which are dual to Koebe polyhedra; the latter being a discrete analogue of conformal parameterizations of the sphere. By theorem 5 below, this leads to the following definition.

Definition 4. A *discrete minimal surface* is an S-isothermic discrete surface $F : Q \rightarrow \mathbb{R}^3$ which satisfies the condition below.

Suppose $x \in Q$ is a white vertex of the quad-graph Q such that $F(x)$ is the center of a sphere. Let $y_1 \dots y_{2n}$ be the vertices neighboring x in Q . (Generically, $n = 2$.) Then $F(y_j)$ are the points of contact with the neighboring spheres and simultaneously points of intersection with the orthogonal circles. Let $F(y_j) = F(x) + b_j$. (See figure 10.) Then the following equivalent conditions hold:

- (i) The points $F(x) + (-1)^j b_j$ lie on a circle.
- (ii) There is an $N \in \mathbb{R}^3$ such that $(-1)^j (b_j, N)$ is the same for $j = 1, \dots, 2n$.
- (iii) There is plane through $F(x)$ such that the points $\{F(y_j) \mid j \text{ even}\}$ and the points $\{F(y_j) \mid j \text{ odd}\}$ lie in planes which are parallel to it at the same distance on opposite sides.

Examples. Fig. 1 (*left*) shows a discrete minimal Enneper surface. Only the circles are shown. A variant of the discrete minimal Enneper surface is shown in figure 13. Here, only the touching spheres are shown. Fig. 1 (*right*) shows a discrete minimal catenoid. Both spheres and circles are shown. Fig. 2 shows a discrete minimal Schwarz-P surface and a discrete minimal Scherk tower.

These examples are discussed in detail in section 7.

Theorem 5. *An S-isothermic discrete surface is a discrete minimal surface, if and only if the dual S-isothermic surface corresponds to a Koebe polyhedron.*

Proof. That the S-isothermic dual of a Koebe polyhedron is a discrete minimal surface is fairly obvious. On the other hand, let $F : Q \rightarrow \mathbb{R}^3$ be a discrete minimal surface and let $x \in Q$ and $y_1 \dots y_{2n} \in Q$ be as in Definition 4. Let $\tilde{F} : Q \rightarrow \mathbb{R}^3$ be the dual S-isothermic surface. We need to show that all circles of \tilde{F} lie in one and the same sphere S and that all the spheres of \tilde{F} intersect S orthogonally. It follows immediately from Definition 4 that the points $\tilde{F}(y_1) \dots \tilde{F}(y_{2n})$ lie on a circle c_x in a sphere S_x around $\tilde{F}(x)$. Let S be the sphere which intersects S_x orthogonally in c_x . The orthogonal circles through $\tilde{F}(y_1) \dots \tilde{F}(y_{2n})$ also lie in S . Hence, all spheres of \tilde{F} intersect S orthogonally and all circles of \tilde{F} lie in S . \square

5 Recipe for constructing discrete minimal surfaces

Given a specific continuous minimal surface, how can one construct an analogous discrete minimal surface? In this section we outline the recipe for doing this. Figure 11 illustrates this construction for the Schwarz P-surface. How to construct the examples which are presented in this paper is explained in detail in Section 7.

Step 1: Gauss image of the curvature lines. The Gauss map of the continuous minimal surface maps its curvature lines to the sphere. Obtain a qualitative picture of this image of the curvature lines under the Gauss map. This yields a quad-graph immersed in the sphere. Here, a choice is made as to which vertices will be black and which will be white. Only the combinatorics of this quad graph matter. (Figure 11, *top left*.) Generically, the vertices have degree 4. Exceptional vertices correspond to ends and nodal points of the continuous minimal surface. (In the figure, the corners of the cube are exceptional. They correspond to nodal points of the Schwarz P-surface.) The exceptional vertices may need to be treated specially. For details see section 7.

Step 2: Circle pattern. From the quad graph, construct the corresponding circle pattern. White vertices will correspond to circles, black vertices to intersection points. Usually, the generalized Koebe theorem is evoked to assert existence and Möbius uniqueness of the pattern. The problem of practically calculating the circle pattern is discussed in section 6. Use eventual symmetries to eliminate the Möbius ambiguity.

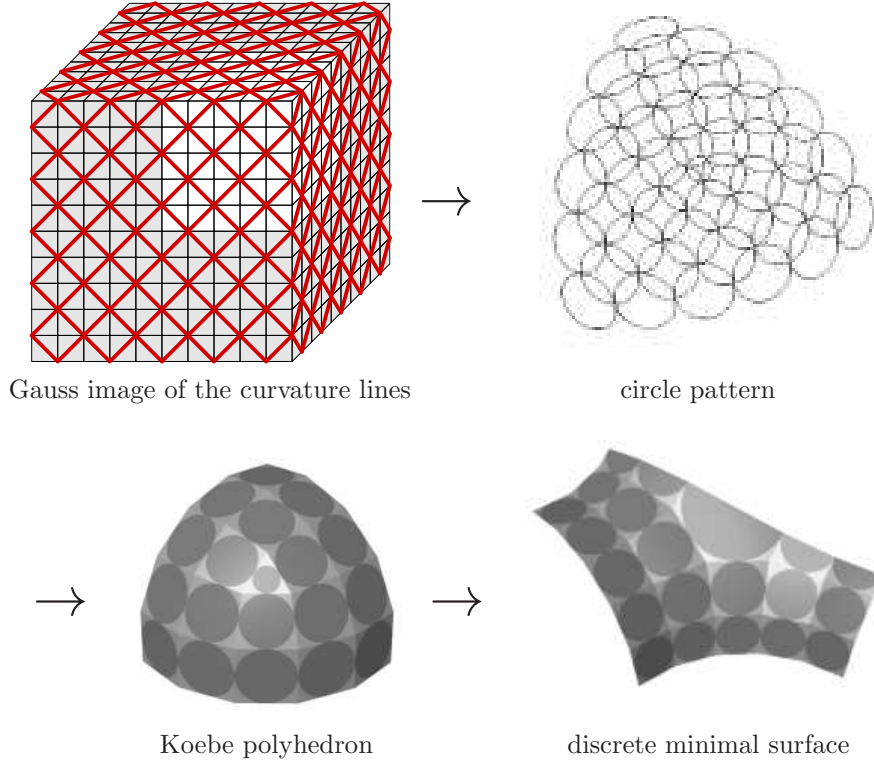


Figure 11: Construction of the discrete Schwarz P-surface.

Step 3: Koebe polyhedron. From the circle pattern, construct the Koebe polyhedron. Here, a choice is made as to which circles will become spheres and which will become circles.

Step 4: Discrete minimal surface. Dualize the Koebe polyhedron to obtain a minimal surface.

6 Orthogonal circle patterns in the sphere

In the simplest cases, like the discrete Enneper surface and the discrete catenoid (Fig. 1), the construction of the corresponding circle patterns in the sphere can be achieved by elementary methods, see Section 7. In general, the problem is not elementary. Developing methods introduced by Colin de Verdière [9], the first and third author have given a constructive proof of the generalized Koebe theorem, which uses a variational principle [5]. It also provides a method for the numerical construction of circle patterns, see also [19]. An alternative algorithm was implemented in Stephenson's program `circlepack` [20]. It is based on methods developed by Thurston [21]. The first step in both methods is to transfer the problem from the sphere to the plane by a stereographic projection. Then the radii of the circles are calculated. If the radii are known, it is easy to reconstruct the circle pattern. The radii are determined by a set

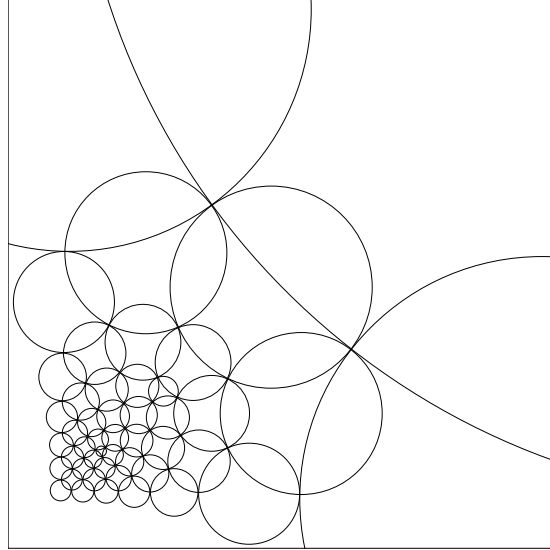


Figure 12: A piece of the circle pattern for a Schwarz-P surface after stereographic projection to the plane.

of nonlinear equations, and the two methods differ in the way in which these equations are solved. Thurston-type methods work by iteratively adjusting the radius of each circle so that the neighboring circles fit around. The above mentioned variational method is based on the observation that the equations for the radii are the equations for a critical point of a convex function of the radii. The variational method involves minimizing this function to solve the equations.

Both of these methods may be used to construct the circle patterns for the discrete Schwarz-P surface and for the discrete Scherk tower, see Figs. 2 and 11. One may also take advantage of the symmetries of the circle patterns and construct only a piece of it (after stereographic projection) as shown in Fig. 12. To this end, one solves the Euclidean circle pattern problem with Neumann boundary conditions: For boundary circles, the nominal angle to be covered by the neighboring circles is prescribed.

However, we actually used an interesting new method to construct the circle patterns for the discrete Schwarz-P surface and the discrete Scherk tower. It is a variational method which works directly on the sphere. No stereographic projection is necessary; the spherical radii of the circles are calculated directly. This variational principle for spherical circle patterns is completely analogous to the variational principles for Euclidean and hyperbolic patterns presented in [5]. We will be brief in its presentation and refer to the above paper for the detailed arguments. Also, we will only treat the case of orthogonally intersecting circles here.

The spherical radius r of a non-degenerate circle in the unit sphere satisfies $0 < r < \pi$. Instead of the radii r of the circles, we use the variables

$$\rho = \log \tan(r/2).$$

For each circle j , we need to find a ρ_j such that the corresponding radii solve

the circle pattern problem. This leads to the following equations, one for each circle. The equation for circle j is

$$(3) \quad 2 \sum_{\text{neighbors } k} (\arctan e^{\rho_k - \rho_j} + \arctan e^{\rho_k + \rho_j}) = \Phi_j,$$

where the sum is taken over all neighboring circles k . For each circle j , Φ_j is the nominal angle covered by the neighboring circles. It is normally 2π for interior circles, but it differs for circles on the boundary or for circles where the pattern branches.

Proposition 4. *The equations (3) are the equations for a critical point of the functional*

$$S(\rho) = \sum_{(j,k)} \left(\operatorname{Im} \operatorname{Li}_2(i e^{\rho_k - \rho_j}) + \operatorname{Im} \operatorname{Li}_2(i e^{\rho_j - \rho_k}) \right. \\ \left. - \operatorname{Im} \operatorname{Li}_2(i e^{\rho_j + \rho_k}) - \operatorname{Im} \operatorname{Li}_2(i e^{-\rho_j - \rho_k}) - \pi(\rho_j + \rho_k) \right) + \sum_j \Phi_j \rho_j.$$

Here, the first sum is taken over all pairs (j, k) of neighboring circles, the second sum is taken over all circles j , and the dilogarithm function $\operatorname{Li}_2(z)$ is defined by $\operatorname{Li}_2(z) = -\int_0^z \log(1 - \zeta) d\zeta / \zeta$.

Unfortunately, the functional $S(\rho)$ is not convex. In fact, its second derivative is the quadratic form

$$D^2 S = \sum_{(j,k)} \left(\frac{1}{\cosh(\rho_k - \rho_j)} (d\rho_k - d\rho_j)^2 - \frac{1}{\cosh(\rho_k + \rho_j)} (d\rho_k + d\rho_j)^2 \right),$$

where the sum is taken over pairs of neighboring circles. The quadratic form is negative for the tangent vector $v = \sum_j \partial / \partial \rho_j$, the index is therefore at least 1. Define a reduced functional $\tilde{S}(\rho)$ by maximizing in the direction v :

$$\tilde{S}(\rho) = \max_t S(\rho + tv).$$

Obviously, $\tilde{S}(\rho)$ is invariant under translations in the direction v . Now the idea is to minimize $\tilde{S}(\rho)$ restricted to $\sum_j \rho_j = 0$. This method has proved to be amazingly powerful. In particular, it can be used to produce branched circle patterns in the sphere.

7 Examples

There are some orthogonal circle patterns with infinitely many circles in the plane that can be constructed explicitly. These include of course the pattern with all circles of equal radius, but also a discrete version of the complex exponential map and a discrete version of z^γ . From these circle patterns one obtains, by projecting stereographically to the sphere and dualizing, discrete minimal versions of Enneper's surface, the catenoid, and variants of Enneper's surface, the m-Enneper surfaces.

Discrete versions of the Schwarz-P surface and the Scherk tower, on the other hand, are obtained by circle patterns with finitely many circles. Their existence follows from Koebe's theorem.

7.1 Enneper's surface

The simplest infinite orthogonal circle pattern in the plane consists of circles with equal radius r and centers on a square grid with spacing $\frac{1}{2}\sqrt{2}r$. Project it stereographically to the sphere, construct orthogonal spheres through half of the circles and dualize to obtain a discrete version of Enneper's surface. See Figs. 1 (*left*) and 18.

7.2 The catenoid

The next most simple example is a discrete version of the catenoid. The underlying circle pattern in the plane is a discretization of the exponential map, the S-Exp pattern introduced in [4]. The underlying quad-graph is \mathbb{Z}^2 , with circles corresponding to points (m, n) with $m + n \equiv 0 \pmod{2}$. The centers $c(m, n)$ and the radii $r(n, m)$ of the circles are

$$c(n, m) = e^{\alpha n + i\rho m}, \quad r(n, m) = \sin(\rho)|c(n, m)|,$$

where

$$\rho = \pi/N, \quad \alpha = \operatorname{arctanh}\left(\frac{1}{2}|1 - e^{2i\rho}|\right).$$

(It is *not* true that $c(m, n)$ is an intersection point if $m + n \equiv 1 \pmod{2}$.)

The corresponding S-isothermic minimal surface is shown in Fig. 1 (*right*). The associated family of the discrete catenoid (see Section 9) is shown in Figs 17.

There are other discrete versions of the catenoid. A discrete isothermic catenoid is constructed in [3]. This construction can be generalized in such a way that one obtains the discrete S-isothermic catenoid described above. This works only because the surface is so particularly simple.

Then, there is the discrete catenoid constructed in [15]. It is an area minimizing polyhedral surface. This catenoid is not related to the S-isothermic catenoid.

7.3 The higher order Enneper surfaces

As the next example, consider the higher order Enneper surfaces [11]. Their Weierstrass data has z^a in place of z . One may think of them as Enneper surfaces with an umbilic point in the center.

An orthogonal circle pattern analogue of the maps z^a was introduced in [4]. Sectors of these circle patterns were proven to be embedded [2], [1]. Stereographic projection to the sphere followed by dualization leads to S-isothermic analogues of the higher order Enneper surfaces. An S-isothermic higher order Enneper surface with $a = 4/3$ (a simple umbilic point) is shown in Fig. 13.

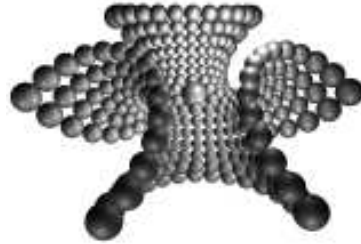


Figure 13: An S-isothermic higher order Enneper surface. The spheres are shown.

7.4 The Schwarz-P surface

The Schwarz-P surface is a triply periodic minimal surface. It is the symmetric case in a 2-parameter family of minimal surfaces with 3 different hole sizes

(only the ratios of the hole sizes matter), see [11]. The domain of the Schwarz-P surface, where the translation periods are factored out, is a Riemann surface of genus 3. The Gauss map is a double cover of the sphere with 8 branch points. The image of the curvature line pattern under the Gauss map is shown schematically in Fig. 11 (*top left*), thin lines. It is a refined cube. More generally, one may consider three different numbers m , n , and k of slices in the three directions. The 8 corners of the cube correspond to the branch points of the Gauss map. Hence, not 3 but 6 edges are incident with each corner vertex. The corner vertices are assigned the label \textcircled{c} . We assume that the numbers m , n , and k are even, so that the vertices of the quad graph may be labelled ' \textcircled{c} ', ' \textcircled{s} ', and ' \bullet ' consistently (see Section 2).

To invoke Koebe's theorem (in the form of Theorem 2), forget momentarily that we are dealing with a double cover of the sphere. Koebe's theorem implies the existence and Möbius-uniqueness of a circle pattern as shown in Fig. 11 (*top right*). (Only one eighth of the complete spherical pattern is shown.) The Möbius ambiguity is eliminated by imposing octahedral metric symmetry.

Now lift the circle pattern to the branched cover, construct the Koebe polyhedron and dualize it to obtain the Schwarz-P surface; see Fig. 11 (*bottom row*). A fundamental piece of the surface is shown in Fig. 2 (*left*).

We summarize these results in a theorem.

Theorem 6. *Given three even positive integers m , n , k , there exists a corresponding unique (unsymmetric) S -isothermic Schwarz-P surface.*

Surfaces with the same ratios $m : n : k$ are different discretizations of the same continuous Schwarz-P surface. The cases with $m = n = k$ correspond to the symmetric Schwarz-P surface.

7.5 The Scherk tower

Finally, consider Scherk's saddle tower, a simply periodic minimal surface, which is asymptotic to two intersecting planes. There is a 1-parameter family, the parameter corresponding to the angle between the asymptotic planes, see [11]. An S -isothermic minimal Scherk tower is shown in Fig. 2 (*right*).

When mapped to the sphere by the Gauss map, the curvature lines of the Scherk tower form a pattern with four special points, which correspond to the four half-planar ends. A loop around a special point corresponds to a period of the surface. In a neighborhood of each special point, the pattern of curvature lines behaves like the image of the standard coordinate net under the map $z \mapsto z^2$ around $z = 0$. In the discrete setting, the special points are modeled by pairs of 3-valent vertices; see Fig. 14 (*left*). This is motivated by the discrete version of z^2 in [2]. The quad graph we use to construct the Scherk tower looks like the quad graph for an unsymmetric Schwarz-P surface with one of the discrete parameters equal to 2. The ratio $m : n$ corresponds to the parameter of the smooth case. Again, by Koebe's theorem, there exists a corresponding circle pattern, which is made unique by imposing metric octahedral symmetry. But now we interpret the special vertices differently. Here, they are not branch points. The right hand side of Fig. 14 shows how they are to be treated: Split the vertex (and edges) between each pair of 3-valent vertices in two. Then introduce new 2-valent vertices between the doubled vertices. Thus, instead of pairs of 3-valent vertices we now have 2-valent vertices. The newly inserted edges have

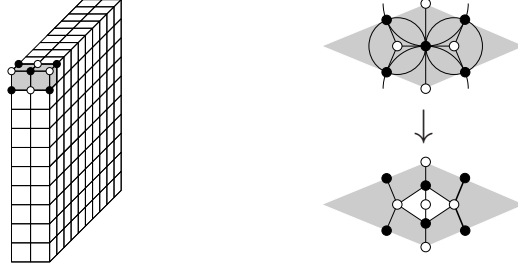


Figure 14: The combinatorics of the Scherk tower.

length 0. Thus, stretching the concept a little bit, one obtains infinite edges after dualization. This is in line with the fact that the special points correspond to half-planar ends.

Fig. 2 (*right*) shows an S-isothermic Scherk tower.

Theorem 7. *Given two even positive integers m and n there exists a corresponding unique S-isothermic Scherk tower.*

The cases with $m = n$ correspond to the most symmetric Scherk tower, the asymptotic planes of which intersect orthogonally.

8 A Weierstrass-type representation

In the classical theory of minimal surfaces, the Weierstrass representation allows the construction of an arbitrary minimal surface from holomorphic data on the underlying Riemann surface. In Section 5, we described a four-step method to construct S-isothermic minimal surfaces. We will now derive a formula, equation (4), for these surfaces that resembles the Weierstrass representation formula. An orthogonal circle pattern in the plane plays the role of the holomorphic data. The formula describes the S-isothermic minimal surface that is obtained by projecting the pattern stereographically to the sphere and dualizing the corresponding Koebe polyhedron.

Theorem 8 (Weierstrass representation). *Let Q be an S-quad-graph, and let $c : Q \rightarrow \mathbb{C}$ be an orthogonal circle pattern in the plane: For white vertices $x \in Q$, $c(x)$ is the center of the corresponding circle, and for black vertices $y \in Q$, $c(y)$ is the corresponding intersection point. The S-isothermic minimal surface*

$$F : \{x \in Q \mid x \text{ is labelled } \textcircled{S}\} \rightarrow \mathbb{R}^3,$$

$$F(x) = \text{the center of the sphere corresponding to } x$$

that corresponds to this circle pattern is given by the following formula. Let $x_1, x_2 \in Q$ be two vertices, both labelled \textcircled{S} , that correspond to touching circles of the pattern, and let $y \in Q$ be the black vertex between x_1 and x_2 , which corresponds to the point of contact. The centers $F(x_1)$ and $F(x_2)$ of the corre-

sponding touching spheres of the S -isothermic minimal surface F satisfy

$$(4) \quad F(x_2) - F(x_1) = \pm \operatorname{Re} \left(\frac{R(x_2) + R(x_1)}{1 + |p|^2} \frac{\overline{c(x_2)} - \overline{c(x_1)}}{|c(x_2) - c(x_1)|} \begin{pmatrix} 1 - p^2 \\ i(1 + p^2) \\ 2p \end{pmatrix} \right),$$

where $p = c(y)$ and the radii $R(x_j)$ of the spheres are

$$(5) \quad R(x_j) = \left| \frac{1 + |c(x_j)|^2 - |c(x_j) - p|^2}{2|c(x_j) - p|} \right|$$

The sign on the right hand side of equation (4) depends on whether the two edges of the quad-graph connecting x_1 with y and y with x_2 are labelled ‘+’ or ‘−’ (see Figs. 4 and 6).

Proof. Let $s : \mathbb{C} \rightarrow S^2 \subset \mathbb{R}^3$ be the stereographic projection

$$s(p) = \frac{1}{1 + |p|^2} \begin{pmatrix} 2 \operatorname{Re} p \\ 2 \operatorname{Im} p \\ |p|^2 - 1 \end{pmatrix}.$$

Its differential is

$$ds_p(v) = \operatorname{Re} \left(\frac{2\bar{v}}{(1 + |p|^2)^2} \begin{pmatrix} 1 - p^2 \\ i(1 + p^2) \\ 2p \end{pmatrix} \right),$$

and

$$\|ds_p(v)\| = \frac{2|v|}{1 + |p|^2},$$

where $\|\cdot\|$ denotes the Euclidean norm.

The edge between $F(x_1)$ and $F(x_2)$ of F has length $R_1 + R_2$ (this is obvious) and is parallel to $ds_p(c(x_2) - c(x_1))$. Indeed, this edge is parallel to the corresponding edge of the Koebe polyhedron, which, in turn, is tangential to the orthogonal circles in the unit sphere, touching in $c(p)$. The pre-images of these circles in the plane touch in p , and the contact direction is $c(x_2) - c(x_1)$. Hence, equation (4) follows from

$$F(x_2) - F(x_1) = \pm (R(x_2) + R(x_1)) \frac{ds_p(c(x_2) - c(x_1))}{\|ds_p(c(x_2) - c(x_1))\|}.$$

To show equation (5), note that the stereographic projection s is the restriction of the reflection on the sphere around the north pole N of S^2 with radius $\sqrt{2}$, restricted to the equatorial plane \mathbb{C} . See Fig. 15. We denote this reflection also by s . Consider the sphere with center $c(x_j)$ and radius $r = |c(x_j) - p|$, which intersects the equatorial plane orthogonally in the circle of the planar pattern corresponding to x_j . This sphere intersects the ray from the north pole N through $c(x_j)$ orthogonally at the distances $d \pm r$ from N , where d , the distance between N and $c(x_j)$, satisfies $d^2 = 1 + |c(x_j)|^2$. This sphere is mapped

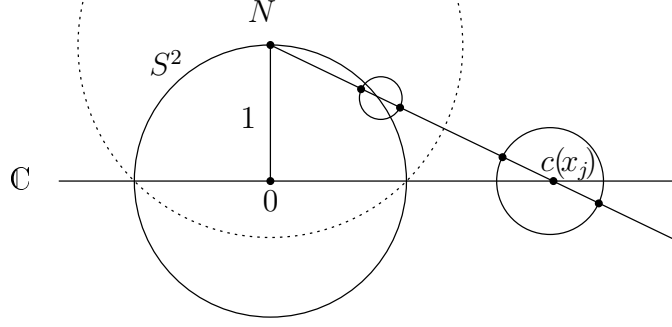


Figure 15: How to derive equation (5).

by s to a sphere, which belongs to the Koebe polyhedron and has radius $1/R_j$. It intersects the ray orthogonally at the distances $2/(d \pm r)$. Hence, its radius is

$$1/R_j = \left| \frac{2r}{d^2 - r^2} \right|.$$

Equation (5) follows. \square

9 The associated family

Every continuous minimal surface comes with an associated family of isometric minimal surfaces with the same Gauss map. Catenoid and helicoid are members of the same associated family of minimal surfaces. The concept of an associated family carries over to discrete minimal surfaces. In the smooth case, the members of the associated family remain conformally, but not isothermally, parametrized. Similarly, in the discrete case, one obtains discrete surfaces which are not S-isothermic but should be considered as discrete conformally parametrized minimal surfaces. We will elaborate on this point below.

The *associated family* of an S-isothermic minimal surface consists of the one-parameter family of discrete surfaces that are obtained by the following construction. Before dualizing the Koebe-polyhedron (which would yield the S-isothermic minimal surface), rotate each edge by an equal angle in the plane which is tangent to the unit sphere in the point where the edge touches the unit sphere.

This construction leads to well defined surfaces because of the following lemma, which is an extension of Lemma 3. See Fig. 16.

Lemma 4. *Let P be a planar polygon with an even number of cyclically ordered edges given by the vectors $l_1, \dots, l_{2n} \in \mathbb{R}^3$, $l_1 + \dots + l_{2n} = 0$. Suppose the polygon has an inscribed circle c with radius R , which lies in a sphere S . Let r_j be the distances from the vertices of P to the nearest touching point on the circle: $\|l_j\| = r_j + r_{j+1}$. Rotate each vector l_j by an equal angle φ in the plane which is tangent to S in the point where the edge touches the unit sphere to obtain the vectors $l_1^{(\varphi)}, \dots, l_{2n}^{(\varphi)}$. Then the vectors $l_1^{(\varphi)*}, \dots, l_{2n}^{(\varphi)*}$ given by*

$$l_j^{(\varphi)*} = (-1)^j \frac{1}{r_j r_{j+1}} l_j^{(\varphi)}$$

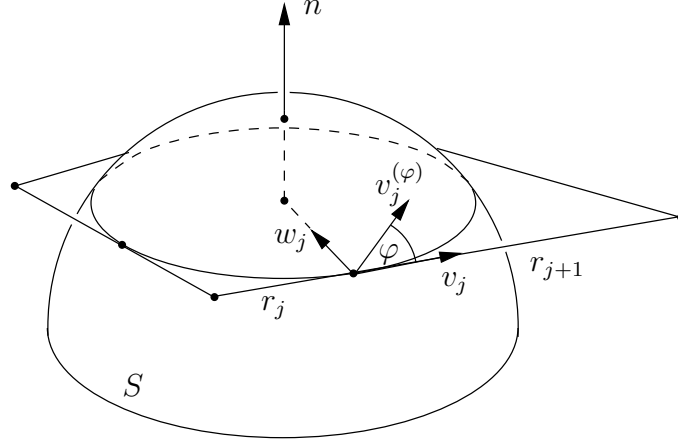


Figure 16: Proof of Lemma 4.

satisfy $l_1^{(\varphi)*} + \dots + l_{2n}^{(\varphi)*} = 0$; that is, they form a (non-planar) polygon.

Proof. For $j = 1, \dots, 2n$ let (v_j, w_j, n) be the orthonormal basis of \mathbb{R}^3 which is formed by $v_j = l_j / \|l_j\|$, the unit normal n to the plane of the polygon P , and

$$(6) \quad w_j = n \times v_j.$$

Let $v_j^{(\varphi)}$ be v_j , rotated by the angle φ in the plane which is tangent to the sphere in the point where the j^{th} edge touches it. Then

$$v_j^{(\varphi)} = \cos \varphi v_j + \sin \varphi \cos \theta w_j + \sin \varphi \sin \theta n,$$

where θ is the angle between the tangent plane and the plane of the polygon. This angle is the same for all edges. Since

$$l_j^{(\varphi)*} = (-1)^j \left(\frac{1}{r_j} + \frac{1}{r_{j+1}} \right) v_j^{(\varphi)},$$

we have to show that

$$\sum_{j=1}^{2n} (-1)^j \left(\frac{1}{r_j} + \frac{1}{r_{j+1}} \right) (\cos \varphi v_j + \sin \varphi \cos \theta w_j + \sin \varphi \sin \theta n) = 0.$$

By Lemma 3,

$$\sum_{j=1}^{2n} (-1)^j \left(\frac{1}{r_j} + \frac{1}{r_{j+1}} \right) v_j = 0.$$

Due to (6),

$$\sum_{j=1}^{2n} (-1)^j \left(\frac{1}{r_j} + \frac{1}{r_{j+1}} \right) w_j = 0$$

as well. Finally,

$$\sum_{j=1}^{2n} (-1)^j \left(\frac{1}{r_j} + \frac{1}{r_{j+1}} \right) n = 0,$$

because it is a telescopic sum. □

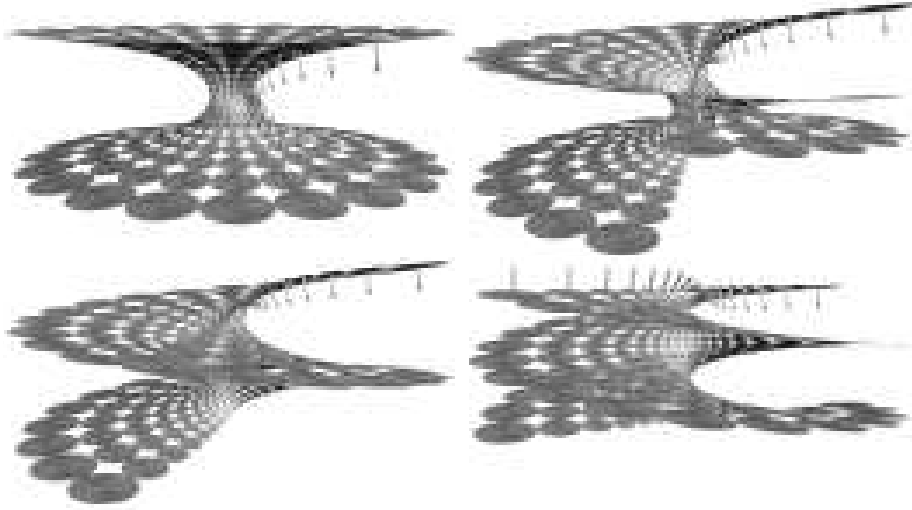


Figure 17: The associated family of the S-isothermic catenoid. The Gauss map is preserved

The following two theorems are easy to prove. First, the Weierstrass-type formula of Theorem 8 may be extended to the associate family.

Theorem 9. *Using the notation of Theorem 8, the discrete surfaces F_φ of the associated family satisfy*

$$F_\varphi(x_2) - F_\varphi(x_1) = \pm \operatorname{Re} \left(e^{i\varphi} \frac{R(x_2) + R(x_1)}{1 + |p|^2} \frac{\overline{c(x_2)} - \overline{c(x_1)}}{|c(x_2) - c(x_1)|} \begin{pmatrix} 1 - p^2 \\ i(1 + p^2) \\ 2p \end{pmatrix} \right),$$

Fig. 17 shows the associated family of the S-isothermic catenoid. The essential properties of the associated family of a continuous minimal surface—that the surfaces are isometric and have the same Gauss map—carries over to the discrete setting in the following form.

Theorem 10. *The surfaces F_φ of the associated family of an S-isothermic minimal surface F_0 consist, like F_0 , of touching spheres. The radii of the spheres do not depend on φ .*

In the generic case, when the quad-graph has \mathbb{Z}^2 -combinatorics, there are also circles through the points of contact, like it is the case with F_0 . The normals of the circles do not depend on φ .

The circles and spheres of F_φ intersect under the angle $\frac{\pi}{2} - \varphi$.

The last statement of the theorem suggests that, while not being S-isothermic, the members of the associated family should be viewed as discrete analogues of isothermic surfaces which are conformally parametrized in such a way that the parameter lines intersect the curvature lines at a constant angle.



Figure 18: A sequence of S-isothermic minimal Enneper surfaces in different discretizations.

10 Convergence

Schramm has proved the convergence of circle patterns with the combinatorics of the square grid to meromorphic functions [18]. Together with the Weierstrass-type representation formula for S-isothermic minimal surfaces, this implies the following approximation theorem for discrete minimal surfaces.

Theorem 11. *Let $D \subset \mathbb{C}$ be a simply connected bounded domain with smooth boundary, and let $W \subset \mathbb{C}$ be an open set that contains the closure of D . Suppose that $F : W \rightarrow \mathbb{R}^3$ is a minimal immersion without umbilic points in conformal curvature line coordinates. There exists a sequence of S-isothermic minimal surfaces $\hat{F}_n : Q_n \rightarrow \mathbb{R}^3$ such that the following holds. Each Q_n is a simply connected S-quad-graph in D which is a subset of the lattice $\frac{1}{n}\mathbb{Z}^2$. If, for $x \in D$, we define $\hat{F}_n(x)$ to be the value of F_n at a point of Q_n closest to x , then \hat{F}_n converges to F uniformly with error $O(\frac{1}{n})$ on compacts in D . In fact, the whole associated families $\hat{F}_{n,\varphi}$ converge to the associated family F_φ of F uniformly (also in φ) and with error $O(\frac{1}{n})$ on compacts in D .*

Proof. Assuming that F is appropriately scaled,

$$F = \operatorname{Re} \int \left(\frac{1 - g(z)^2}{i(1 + g(z)^2)} \right) \frac{dz}{g'(z)},$$

where $g : W \rightarrow \mathbb{C}$ is a locally injective meromorphic function. By Schramm's results (Theorem 9.1 of [18] and the remark on p. 387), there exists a sequence of orthogonal circle patterns $c_n : Q_n \rightarrow \mathbb{C}$ approximating g and g' uniformly and with error $O(\frac{1}{n})$ on compacts in D . Define F_n by the Weierstrass formula (4) with data $c = c_n$. Using the notation of Theorem 8, one finds

$$\frac{1}{n^2} (F_n(x_2) - F_n(x_1)) \xrightarrow{n \rightarrow \infty} \frac{1}{n} \left(\frac{1 - g(y)^2}{i(1 + g(y)^2)} \right) \frac{1}{g'(y)} + O\left(\frac{1}{n^2}\right)$$

uniformly on compacts in D . Setting $\hat{F}_n = \frac{1}{n^2} F_n$, the convergence claim follows. The same reasoning applies to the whole associated family of F . \square

Fig. 18 illustrates the convergence of S-isothermic Enneper surfaces to the continuous Enneper surface.

References

- [1] S. I. Agafonov, Imbedded circle patterns with the combinatorics of the square grid and discrete Painlevé equations, *Discrete Comput. Geom.* **29** (2003), no. 2, 305–319.
- [2] S. I. Agafonov and A. I. Bobenko, Discrete Z^γ and Painlevé equations, *Internat. Math. Res. Notices* **2000**, no. 4, 165–193.
- [3] A. I. Bobenko and U. Pinkall, Discrete isothermic surfaces, *J. reine angew. Math.* **475** (1996), 187–208.
- [4] A. I. Bobenko and U. Pinkall, Discretization of surfaces and integrable systems, in A. I. Bobenko and R. Seiler, *Discrete Integrable Geometry and Physics*, Clarendon Press, Oxford, 1999, pp. 3–58.
- [5] A. I. Bobenko and B. A. Springborn, Variational principles for circle patterns and Koebe’s theorem, [arXiv:math.GT/0203250](https://arxiv.org/abs/math.GT/0203250) (2002), to appear in *Trans. Amer. Math. Soc.*
- [6] G. R. Brightwell and E. R. Scheinerman, Representations of planar graphs, *SIAM J. Disc. Math.* **6**(2) (1993), 214–229.
- [7] R. L. Bryant, Surfaces of mean curvature one in hyperbolic space, *Astérisque* **154–155** (1987).
- [8] E. Christoffel, Ueber einige allgemeine Eigenschaften der Minimumsflächen, *J. Reine Angew. Math.* **67** (1867), 218–228.
- [9] Y. Colin de Verdière, Un principe variationnel pour les empilements de cercles, *Invent. Math.* **104** (1991), 655–669.
- [10] P. Collin, L. Hauswirth and H. Rosenberg, The geometry of finite topology Bryant surfaces, *Ann. of Math.* **153** (2001), 623–659.
- [11] U. Dierkes, S. Hildebrandt, A. Küster and O. Wohlrab, *Minimal Surfaces I*, Springer-Verlag, Berlin, 1992.
- [12] Zh. He and O. Schramm, The C^∞ -convergence of hexagonal disk packings to the Riemann map, *Acta. Math.* **180** (1998), 219–245.
- [13] D. Hoffman and H. Karcher, Complete embedded minimal surfaces of finite total curvature, in: R. Osserman (editor), *Geometry V: Minimal surfaces*, Encyclopaedia of Mathematical Sciences, volume 90, Springer-Verlag, Berlin, 1997, pp. 5–93.
- [14] P. Koebe, Kontaktprobleme der konformen Abbildung, *Abh. Sächs. Akad. Wiss. Leipzig Math.-Natur. Kl.* **88** (1936), 141–164.
- [15] K. Polthier and W. Rossman, Discrete constant mean curvature surfaces and their index, *J. reine angew. Math.* **549** (2002), 47–77.
- [16] I. Rivin, A characterization of ideal polyhedra in hyperbolic 3-space, *Ann. of Math.* **143** (1996), 51–70.
- [17] O. Schramm, How to cage an egg, *Duke Math. J.* **86** (1997), 347–389.

- [18] O. Schramm, Circle patterns with the combinatorics of the square grid, *Invent. Math.* **107**(3) (1992), 543–560.
- [19] B. A. Springborn, Constructing circle patterns using a new functional, to appear in Chr. Hege and K. Polthier (eds.), *Visualization and Mathematics III*, Proceedings of the International Workshop on Visualization and Mathematics 2002 in Berlin, Springer-Verlag, Berlin.
- [20] K. Stephenson, Circle packing: Experiments in discrete analytic function theory, *Experiment. Math.* **4** (1995), 307–348.
- [21] W. P. Thurston, The geometry and topology of three-manifolds, an electronic version is currently provided by the MSRI at the URL <http://www.msri.org/publications/books/gt3m>.

Alexander I. Bobenko

Technische Universität Berlin
 Institut für Mathematik, Sekr. MA 8-5
 Strasse des 17. Juni 136
 10623 Berlin, Germany
 email: bobenko@math.tu-berlin.de

Tim Hoffmann

Department of Mathematics and Statistics
 Lederle Graduate Research Tower
 University of Massachusetts
 Amherst, MA 01003-4515, USA
 email: timh@math.umass.edu

Boris A. Springborn

Technische Universität Berlin
 Institut für Mathematik, Sekr. MA 8-5
 Strasse des 17. Juni 136
 10623 Berlin, Germany
 email: springb@math.tu-berlin.de